

Searching for New Physics Through AMO Precision Measurements

Chad Orzel

Union College Department of Physics and Astronomy, Science and Engineering Center, Schenectady, NY 12308 USA

E-mail: orzeltc@union.edu

Abstract. We briefly review recent experiments in atomic, molecular, and optical physics using precision measurements to search for physics beyond the Standard Model. We consider three main categories of experiments: searches for changes in fundamental constants, measurements of the anomalous magnetic moment of the electron, and searches for an electric dipole moment of the electron.

1. Introduction

Most physicists asked to think of searches for physics beyond the Standard Model immediately picture multi-billion dollar particle accelerators with detectors the size of office buildings, or gigantic astrophysical detectors in remote locations. This is a natural assumption, as very high energies are required to produce and detect exotic particles associated with new physics. At lower energies, interactions with these particles are very weak, and thus they have little effect on physics at typical atomic energy scales of a few electron volts.

In fact, though, in labs around the world, new physics searches are underway using atoms and molecules. These experiments, to borrow a phrase from Gerald Gabrielse of Harvard, search for new physics using precision, rather than energy. While the effects of new physics at atomic energy scales are tiny, modern laser spectroscopy allows measurements of astonishing precision, sufficient to detect the subtle influence of new fundamental physics.

In this paper, we give a brief review of the essential techniques involved in AMO precision measurements, then look at three types of new-physics searches through precision measurement: the use of atomic clocks to look for changes in fundamental constants, measurements of the anomalous magnetic moment of the electron, and searches for a permanent electric dipole moment of the electron.

2. Precision Spectroscopy

The general problem of precision spectroscopy is to find the frequency of light needed to drive the transition between two quantum states. For extremely precise measurements, these must be states with a small natural linewidth due to spontaneous emission; pairs of atomic hyperfine states, or dipole-forbidden transitions are typical. In addition to the two states being studied, there must be a state-selective detection method, typically involving laser excitation via a dipole-allowed transition to another state and detection of the resulting fluorescence.

In the last several decades, methods of precision spectroscopy have advanced to the point where transition frequencies can be determined at the level of a few parts in 10^{18} , sufficient to resolve possible contributions from physics beyond the Standard Model. This level of precision relies on two principal tools: the Ramsey separated-fields method of spectroscopy, and the femtosecond laser frequency comb. In this section, we will briefly review these tools, before moving on to discuss the experiments that apply them.

2.1. Ramsey Interferometry

Ultimately, AMO precision measurement techniques can be traced to the development of highly accurate atomic clocks. The laser-cooled cesium clocks that are presently used as primary time standards are stable to within a few parts in 10^{16} [1] and improvements of an order of magnitude or more have been demonstrated with experimental clocks based on other atoms. All of these clocks are based on the separated-field spectroscopy method developed by Norman Ramsey in 1950[2], and most AMO precision measurements use some version of the Ramsey technique, so we briefly review it here.

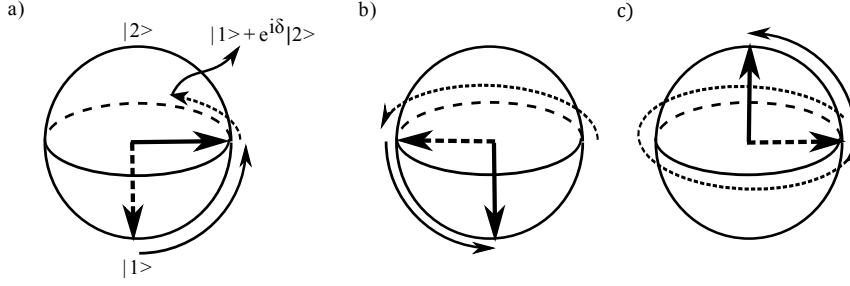


Figure 1. Bloch sphere visualization of the Ramsey spectroscopy sequence. a) The initial $\pi/2$ pulse rotates the state vector into a superposition state, which begins to precess about the axis at a frequency $(\omega - \omega_0)$. b) After a half-integer number of rotations, the second $\pi/2$ pulse rotates the state vector back to state $|1\rangle$. c) After an integer number of rotations, the second $\pi/2$ pulse completes the transition to state $|2\rangle$.

In Ramsey interferometry, a system in state $|1\rangle$ is first exposed to light at frequency ω near the resonant frequency ω_0 , which drives coherent Rabi oscillations between $|1\rangle$ and $|2\rangle$ at a frequency Ω . The intensity and duration of the pulse are chosen to prepare the system in a coherent superposition of $|1\rangle$ and $|2\rangle$ (a “ $\pi/2$ -pulse”). The superposition evolves freely for a time T , then is exposed to a second $\pi/2$ pulse. At the end of this pulse sequence, the state of the system is probed to determine whether it has made a transition to $|2\rangle$.

The transition probability at the end of this sequence is

$$P(1 \rightarrow 2) = \left(\frac{\Omega \tau_{\pi/2}}{2} \right)^2 \left[\frac{\sin \left(\frac{\omega - \omega_0}{2} \tau_{\pi/2} \right)}{\left(\frac{\omega - \omega_0}{2} \tau_{\pi/2} \right)} \right]^2 \cos^2 \left(\frac{(\omega - \omega_0) T}{2} \right)$$

This consists of an overall amplitude depending on the Rabi frequency Ω and the pulse duration $\tau_{\pi/2}$ and a rapid oscillation depending on the free evolution time T . The width in frequency of one of these “Ramsey fringes” is $\Delta\omega = \frac{\pi}{T}$, inversely proportional to the free evolution time T . This is what gives the Ramsey method its extreme sensitivity: for laser-cooled Cs clocks, $T \sim 1$ s[1], allowing frequency resolution of less than 1Hz on the 9.19GHz transition between Cs hyperfine ground states that defines the SI second.

The Ramsey fringes arise from interference between the two parts of the initial superposition, whose phases evolve at different rates. An intuitive illustration uses the Bloch sphere picture (Fig.1), in which the state is represented by a vector to a point on the surface of a unit sphere. The states $|1\rangle$ and $|2\rangle$ correspond to the south and north poles of the sphere, with other surface points describing superposition states. A $\pi/2$ pulse corresponds to rotating the state vector by $\pi/2$ about the x-axis, so the initial pulse of the Ramsey sequence rotates the vector from the south pole to the equator of the Bloch sphere, along the +y-axis. If this were followed immediately by the second $\pi/2$ pulse, the state vector would be rotated another $\pi/2$, ending at the north pole (the $|2\rangle$ state).

During the free evolution time, however, the phase of the superposition evolves at a frequency $\omega - \omega_0$ (in the rotating wave approximation), corresponding to precession of the state vector about the z-axis. The result of the second $\pi/2$ pulse thus depends on the position after the free evolution time T . If the state vector has completed

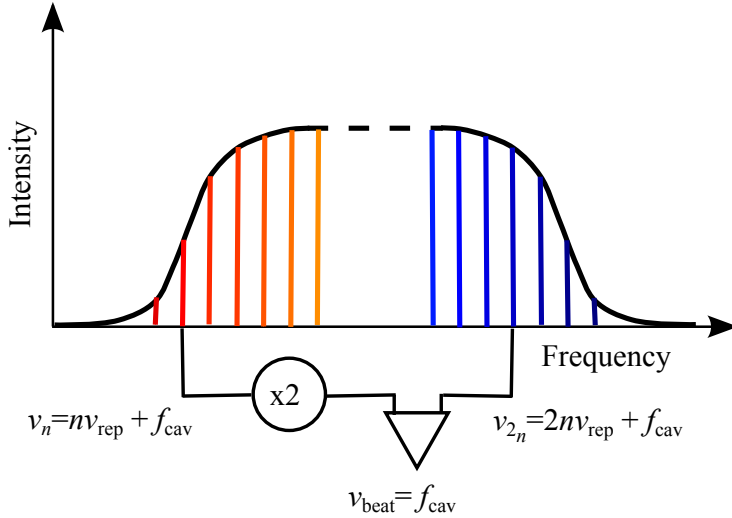


Figure 2. A self-referenced frequency comb. Light from the n^{th} mode is frequency doubled and mixed with light from the $2n^{th}$ mode. The beat frequency is equal to the offset frequency due to cavity dispersion, allowing the absolute determination of any optical frequency in terms of the cavity offset and the repetition rate, both RF frequencies that are easily referenced to microwave frequency standards.

an integer number of rotations, it returns to its initial position, and the second $\pi/2$ rotation completes the transition from $|g\rangle \rightarrow |e\rangle$. If the state vector has completed a half-integer number of rotations, however, the state vector will be along the -y-axis, and the second $\pi/2$ rotation returns it to the south pole, returning the system to the ground state.

The oscillating coherence between the terms of the superposition state, then, is the origin of the T -dependence of the Ramsey fringes. Most AMO precision measurements use some variant of the Ramsey scheme: an initial interaction to prepare a coherent superposition between two states of an atomic or molecular system, followed by a period of free evolution, followed by a second interaction with the light field, then a state measurement, with high frequency resolution enabled by interference between states.

2.2. Optical Frequency Combs

As the SI definition of time is based on the hyperfine ground state splitting in Cs, measurements of absolute frequencies must ultimately be referenced to Cs clocks, but comparing transition frequencies in the optical domain to the microwave Cs frequency has presented a significant technical challenge. In recent years, the development of femtosecond laser frequency combs has greatly simplified such comparisons, leading to a rapid advance to measurements of unprecedented precision[3].

The frequency spectrum of a mode-locked laser consists of a large number of regularly spaced narrow modes (Fig.2) , The n^{th} mode has a frequency

$$\nu_n = n\nu_{rep} + f_{cav}$$

where ν_{rep} is the repetition frequency of the laser (typically ~ 100 MHz), which is controlled by the laser cavity, and f_{cav} is a frequency offset due dispersion in the cavity. The width of the frequency spectrum will be determined by the duration of a single laser pulse, and for pulses a few femtoseconds long, the bandwidth of the comb can span a full octave of frequency. Light from the n^{th} mode can be frequency-doubled and mixed with light from the $2n^{th}$ mode, producing a radio-frequency beat note at the difference frequency:

$$\Delta\nu = 2\nu_n - \nu_{2n} = (2n\nu_{rep} + 2f_{cav}) - (2n\nu_{rep} + f_{cav}) = f_{cav}$$

This comparison directly measures the cavity offset, allowing the absolute determination of the frequency of any mode in terms of RF frequencies that can easily be referenced to a microwave atomic clock. Such a self-referenced frequency comb allows the direct comparison of two different laser frequencies across a wide range: the repetition rate of the comb can be locked to an atomic clock, and the absolute laser frequencies determined from the beat note with the nearest tooth of the comb. Alternatively, the comb can be stabilized to one of the two laser sources (from an optical-frequency atomic clock, for example), and the relative frequency difference determined from the beat note of the second laser.

Frequency combs have found applications in molecular spectroscopy[4], and as reference sources for astronomical spectrometers[5, 6]. Their primary impact, however, has been in precision spectroscopy, where the exceptional precision of comb-based comparisons allows the possibility of frequency metrology to 18 or 19 decimal places, opening many possibilities for new physics searches with AMO techniques.

3. Changing Fundamental Constants

Many theories of attempting combine gravity with the Standard Model predict possible changes in the values of fundamental constants over cosmological time scales[7]. These changes are detectable through variation of dimensionless ratios of constants, the most significant of which are the fine structure constant $\alpha = e^2/4\pi\epsilon_0\hbar c$, which combines the electron charge e , speed of light c and Planck's constant \hbar , and the proton-electron mass ratio $\mu = m_p/m_e$. Changes in these ratios change the relative energies of atomic and nuclear states, reviewed in Ref. [8]; here we will highlight only a few AMO-based searches.

The influence of changing constants on nuclear states is seen primarily through geophysical records of radioactive decay. Isotope ratios from the ‘‘natural nuclear reactor’’ at Oklo provide a fossil record of nuclear reaction rates during its operation 1.7 billion years ago, limiting the possible variation to $-0.11 \times 10^{-7} \leq \Delta\alpha/\alpha \leq 0.22 \times 10^{-7}$ [9]. Iron meteorites containing records of the β -decay of ^{187}Re into ^{187}Os weaker bound, $\Delta\alpha/\alpha = (2.5 \pm 16) \times 10^{-7}$ over 4.6 billion years[10]. Both of these methods are somewhat model-dependent, as the reaction rates depend on the environment in the distant past. Weaker constraints over cosmological time scales are provided by analysis of the cosmic microwave background[11, 12] and primordial nucleosynthesis[13].

For atomic and molecular states, the fractional shift of a transition frequency ω can be written in the general form (following Ref. [23]):

$$\frac{1}{\omega} \frac{\partial\omega}{\partial t} = A \frac{1}{\alpha} \frac{\partial\alpha}{\partial t} + B \frac{1}{\mu} \frac{\partial\mu}{\partial t} + C \frac{1}{g} \frac{\partial g}{\partial t} - \frac{1}{\omega_{Cs}} \frac{\partial\omega_{Cs}}{\partial t} \quad (1)$$

where the numerical factors A, B , and C give the sensitivity of the transition in question to changes in α , μ , and the nuclear g-factor g , respectively. The latter two primarily affect hyperfine transitions, which depend on the interaction between the electron spin and the nuclear magnetic moment. These sensitivity factors vary between different atoms and different transitions within the same atom, and are determined from numerical calculations of atomic or molecular wavefunctions. The final term accounts for the shift in the frequency of the Cs ground-state hyperfine transition, which provides the definition of the SI second, and is itself subject to change with changes in the fundamental constants.

Spectroscopic observations of high-redshift astronomical objects such as quasars and gas clouds provide a direct probe of the history of the fine-structure constant. The general procedure is to compare the observed wavelengths of spectral lines associated with a particular astronomical object (either emission lines in the spectrum of the object itself, or absorption features in the spectrum from a more distant object such as a quasar) to determine whether the spectral lines from an earlier epoch are the same as those for the same system today. This procedure is complicated by the need to account for the cosmological redshift due to the Hubble expansion, so these studies generally look at differences between two or more transitions associated with the same object.

The simplest spectroscopic measurements of the past history of fundamental constants use pairs of lines associated with a single element; for example, Cowie and Songaila[14] measured the difference between fine structure states of Si IV, which scales as α^2 , obtaining a value of $\Delta\alpha/\alpha = (3.3 \pm 5.5) \times 10^{-6}$ at redshifts of $z \sim 1.8$ ($\sim 10 \text{ Gyr}$). Numerous subsequent measurements have had similar sensitivity[15, 16, 17, 18, 19], at redshifts up to $z = 5.2$, some finding significant changes, other consistent with no change.

The most dramatic of these results is the claim by Webb et al.[20, 21] of not only a change over time, but a spatial variation having a dipole pattern:

$$\frac{\Delta\alpha}{\alpha} = Ar \cos \theta$$

where $r = ct(z)$ is the look-back distance in Glyr, θ is the angle from the pole of the dipole pattern, and $A = (1.1 \pm 0.25) \times 10^{-6} \text{ Glyr}^{-1}$. This claim is based on a many-multiplet analysis of data from the Keck and VLT telescopes, using multiple spectral lines of several different elements. Such a dipole pattern might explain the conflict between measurements (depending on the location of the sources on the sky), but it remains controversial[16, 19, 22], and awaits confirmation by independent observations or additional telescopes.

Present-day spectroscopic measurements can not, of course, provide any information about changes over cosmological time scales. They do, however, provide a complementary measurement of the contemporary rates of change, and the exceptional accuracy of modern atomic clocks allows these present-day limits to be competitive with the best astrophysical measurements. A measured frequency shift at the 1ppm level looking back 10^{10} years limits the average rate of change to 10^{-16} yr^{-1} ; an atomic clock with accuracy of a part in 10^{16} , like laser-cooled Cs fountain clocks, needs only one year to match that limit. If the dipole pattern claimed by Webb et al. exists, the motion of the solar system through that background should produce a fractional change of order 10^{-19} yr^{-1} [27], which may be within reach of some AMO experiments (see Fig. 3) .

Reference [23] provides an excellent summary of the history of atomic-clock-based searches for changing constants as of 2007. In this paper, we will focus on more recent measurements that demonstrate the power of precision AMO techniques.

3.1. Microwave Clock Comparisons

Atomic cesium provides the basis of the SI second, defined as 9,192,631,770 oscillations of the light associated with the ground-state hyperfine transition in ^{133}Cs , and laser-cooled fountain clocks now serve as primary frequency standards for most national laboratories. The analogous transition in rubidium, with a frequency of 6.8GHz, has also been studied as a possible time standard, due to some favorable collisional properties. The LNE-SYRTE lab in Paris has been operating an ensemble of fountains, including a dual-species apparatus capable of operating with either Cs or Rb, since 1998. Measurements of the frequency ratio $\eta = \nu_{\text{Rb}}/\nu_{\text{Cs}}$ over the last 14 years [24, 25] provide one of the tightest constraints on modern changes α .

As hyperfine transitions, the Cs and Rb transition frequencies are sensitive not only to changes in α , but also to changes in g and μ as seen in equation 1. The two transitions have the same dependence on μ , though, so the frequency ratio is primarily sensitive to changes in α and weakly sensitive to changes in the g-factors. The 14-year comparison finds a fractional change $\dot{\eta}/\eta = (-1.36 \pm 0.91) \times 10^{-16} \text{yr}^{-1}$. Combining this result with the results of 6 other frequency ratio measurements, which have different sensitivities to the various constants, allows them to separate out the different components, giving $\dot{\alpha}/\alpha = (-0.25 \pm 0.26) \times 10^{-16} \text{yr}^{-1}$ and $\dot{\mu}/\mu = (1.5 \pm 3.0) \times 10^{-16} \text{yr}^{-1}$. These are comparable to the best limits obtained from astrophysical measurements, and are the second-best laboratory limit to date.

The very long observation time for the Rb/Cs comparison also allows tests of other possible sources of variation. Binning their measurements by month, they search for a possible variation with respect to the position of the Earth in its orbit around the Sun, interpreted as a possible coupling to the gravitational potential. They find a limit of $c^2 \frac{1}{\eta} \frac{\partial \eta}{\partial U} = (0.11 \pm 1.04) \times 10^{-6}$, an improvement by a factor of 1.4 over the best previous limit [26]. The Rb-Cs comparison also limits any variation due to passage through a spatial gradient in α to around 10^{-29}m^{-1} , still approximately two orders of magnitude larger than the expected variation [27]. The Rb and Cs clocks are unlikely to improve by this much, but other experiments may reach the necessary sensitivity.

3.2. Optical Clocks

One major area of time standards research over the last 30 years has been the development of time standards operating at optical rather than microwave frequencies. The move from GHz to THz frequencies can, in principle, produce a dramatic increase in the precision of a clock, but numerous technological developments needed to be made for optical clocks to reach their full potential, such as laser sources with sub-Hz linewidths, and optical frequency combs to connect the THz frequencies of optical transitions to lower frequencies that can be compared to current microwave time standards and more easily counted electronically for use as a reference standard.

As these technologies have come together, numerous “optical clock” systems have been proposed and investigated, many of them using single trapped ions [34] such as Hg^+ [28], Yb^+ [29, 30], Sr^+ [31], In^+ [32] and Ca^+ [33]. Trapped ions can be laser cooled to the ground state of the trap, held for long periods allowing long

interaction times with a single ion, and interrogated with high fidelity, making forbidden transitions to long-lived metastable states a promising basis for an optical frequency standard. Trapped-ion clocks in Yb^+ [35] and Hg^+ [36] have been compared to microwave frequency standards in order to place limits on changes in fundamental constants at the $\dot{\alpha}/\alpha \leq 10^{-15}$ level.

The best performance of an optical clock to date is the $^{27}\text{Al}^+$ clock at NIST-Boulder. Unlike most other ion clock systems $^{27}\text{Al}^+$ does not have an allowed transition accessible with current laser technology that can be used for cooling and state detection. The NIST group solve this problem with techniques developed for quantum information processing with trapped ions, by co-trapping the $^{27}\text{Al}^+$ and a “logic ion,” either Be^+ or Mg^+ . They laser cool the logic ion, which sympathetically cools the “clock” ion. They use Raman transitions to map the internal state of the clock ion to that of the logic ion via the common motional state of the two trapped ions, and detect the final state using the laser cooling transition in the logic ion.

This quantum logic spectroscopy was first demonstrated in 2005[37] using the $^1S_0 \rightarrow ^3P_1$ transition, and used to measure the absolute frequency of the $^1S_0 \rightarrow ^3P_0$ clock transition, $\nu = 1\,121\,015\,393\,207\,851(6)\text{Hz}$, in 2007[38]. The initial $^{27}\text{Al}^+$ clock, using Be^+ for the logic ion, was compared to the previously developed $^{199}\text{Hg}^+$. They determined the frequency ratio to a remarkable 17 decimal places by comparing the laser frequencies via a frequency comb:

$$\frac{\nu_{\text{Al}}}{\nu_{\text{Hg}}} = 1.052871833148990438(55) \quad (2)$$

The optical transitions used for the clock states in both $^{27}\text{Al}^+$ and $^{199}\text{Hg}^+$ are sensitive to changes in the fine structure constant (only weakly in Al, but more strongly in Hg), but depend on μ and g only at higher orders, which can be neglected. Eq. 2, then, directly probes the change in α . Repeated measurements of this ratio over the course of one year give the best laboratory limit to date on $\frac{\partial}{\partial t} \ln \alpha = (-1.6 \pm 2.3) \times 10^{-17} \text{yr}^{-1}$ [39].

The NIST group has since constructed a second $^{27}\text{Al}^+$ clock, replacing the Be logic ion with Mg (whose mass is closer to Al allowing for more efficient coupling between the ions), and incorporating some mechanical improvements. These upgrades improve the clock performance by more than a factor of two, from an inaccuracy of 2.3×10^{-17} for the Al-Be clock to 0.86×10^{-17} [40]. Measurement at this level of accuracy opens many possibilities for new physics searches, not only through improved clock comparisons, but through gravitational measurements, as the clock uncertainty is comparable to the gravitational redshift for a change in elevation of $\sim 10\text{cm}$; the NIST group compared the frequencies of their two $^{27}\text{Al}^+$ clocks, and clearly resolved the frequency shift due to raising one 33cm above the other[41].

The other major category of optical frequency clocks use neutral atoms in optical lattices[43]. Lattice clocks offer the advantage of using many atoms rather than a single ion (using multiple ions in a single trap can lead to large frequency shifts due to the Coulomb interaction), but the confining lattice must be operated at a “magic” wavelength where the AC Stark shifts of the two states in the clock transition are identical. The need for a “magic” lattice wavelength limits the atomic species that can be used in a lattice clock, but lattice clocks have been demonstrated in Sr[44, 45, 46], Yb[47, 48], and Hg[49, 50, 51].

The most fully developed of these systems is strontium, with ^{87}Sr lattice clocks operating in Tokyo, Boulder, and Paris since 2006. The measured

transitions frequencies for the $^1S_0 \rightarrow ^3P_0$ clock transition, independently calibrated by comparisons to Cs primary standards, agree to within 1.7Hz out of 429228004229 874 Hz. This comparison limits both the possible change in fundamental constants ($\dot{\alpha}/\alpha = (-3.3 \pm 3.0) \times 10^{-16} yr^{-1}$, $\dot{\mu}/\mu = (1.6 \pm 1.7) \times 10^{-16} yr^{-1}$) and the possible annual variation due to a coupling to gravity[52]. This limit is not as tight as the Hg⁺-Al⁺ comparison, [39], but much of the uncertainty comes from the comparison to the microwave Cs standards. Direct comparisons to other optical frequency standards and improvements in optical clock technology should reduce these uncertainties, as will observations over a longer period of time.

3.3. Other Systems

While existing clock systems place limits on the modern rate of change of fundamental constants, the current sensitivity will need to improve by 1-2 orders of magnitude in order to address the question of the spatial variation seen in quasar data. Improvements in optical clocks may bring this sensitivity within reach, two other dramatically different approaches might also reach the necessary sensitivity.

One method drawing on atomic clock technology is a “nuclear clock” using the low-energy (~ 7.6 eV) isomer transition in ^{229}Th , which it may be possible to excite with VUV lasers[53, 54]. Such a nuclear transition would offer exceptional shielding against external perturbations, to the point where a clock using large numbers of trapped ions[55], or thorium nuclei implanted in a solid crystal of a material such as CaF that is transparent to the excitation light[56] might be feasible. Both trapped-ion and solid-state proposals are estimated to reach accuracies of 10^{-19} . Additionally, the nuclear isomer transition might offer enhanced sensitivity to changes in fundamental constants, though more accurate models will be needed to determine the exact sensitivity[57]. Several groups are working toward laser spectroscopy of the isomer transition, though it has not yet been detected.

The other relatively new method potentially sensitive enough to detect spatial variation in α uses the $4f^{10}5d6s \rightarrow 4f^95d^26s$ transition between two nearly degenerate states of opposite parity in dysprosium[58]. This energy splitting can be measured directly using an allowed dipole transition, and the RF transition frequencies can be counted directly, greatly simplifying the analysis. The energy splitting of the transition is comparable to the isotope shift for Dy, so the frequency shift due to changing α has different sign for different isotopes, removing the need for an explicit comparison to other elements.

An initial measurement comparing the 235MHz transition in ^{162}Dy with the 3.1MHz transition in ^{163}Dy gives a limit of $\dot{\alpha}/\alpha = (-2.7 \pm 2.6) \times 10^{-15} yr^{-1}$ [59]. The eight-month span of this measurement also places a limit on annual variation due to a coupling to gravity[60]. These initial limits are not as good as the best clock comparison data, but the ultimate possible sensitivity may be as high as $\dot{\alpha}/\alpha \sim 10^{-18} yr^{-1}$ [61]. Since those measurements, laser cooling has been demonstrated in Dy, with both boson[62] and fermion[63] isotopes cooled to quantum degeneracy, which may allow further improvements.

The precise sensitivity to changes in α and other fundamental constants depends on the details of atomic and nuclear wavefunctions. Numerical calculations are underway in neutral atoms[64] and highly charged ions[65] to determine other promising candidates for finding new physics through precision measurement.

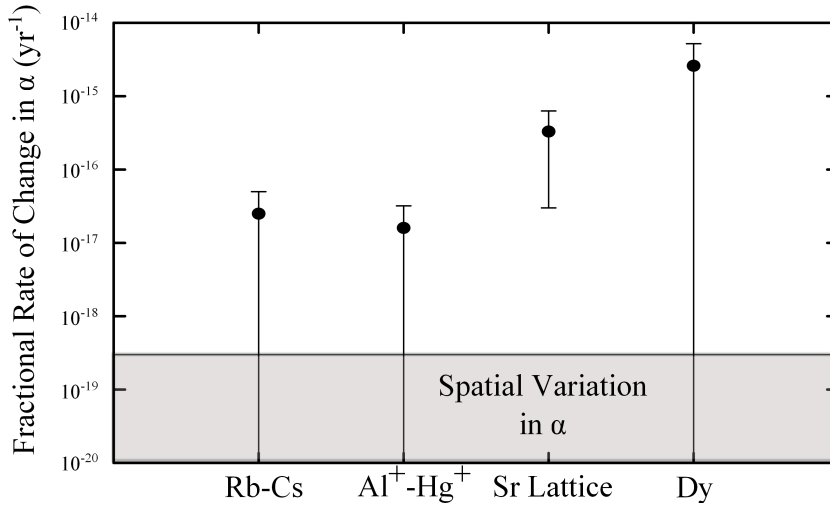


Figure 3. Summary of the best current measurements of $|\dot{\alpha}|/\alpha$ from AMO techniques. The horizontal line indicates the approximate yearly rate of change due to the motion of the Sun through the spatial gradient of Ref. [20]. All the measurements are consistent with $\dot{\alpha} = 0$ at the $1 - \sigma$ level except the Sr lattice clock comparison from Ref. [52].

4. The Value of α

Detecting changes in α is one possible way for AMO techniques to detect new physics, but the absolute value of α can also shed light on possible new physics. A recent measurement of the g -factor that determines the magnetic moment due to the electron's spin $\boldsymbol{\mu} = -g \frac{e}{2m_e} \mathbf{S}$, combined with a tenth-order QED calculation gives the best current measurement of the value of α . A comparison of this value and the best independent measurement of α , based on recoil measurements of Rb atoms, provides the most stringent test of QED to date, and allows clear observation of the muonic and hadronic contributions to the electron g -factor.

4.1. The Electron g -factor

While the techniques used are drawn from precision AMO measurements, the key system in this case is not a naturally occurring atom, but an artificial one: a single electron held in a Penning trap, consisting of an axial magnetic field and an electrostatic quadrupole field[66]. Precision measurement of α uses two sets of quantized states due to the combination of cyclotron motion (cyclotron frequency $\nu_c = (e/2\pi m_e)B_z$) and the interaction between the electron spin and the trap magnetic field. The total energy of the n th cyclotron state is:

$$E_{nm_s} = E_n^{(cyc)} + E_{m_s}^{(spin)} = \left(n + \frac{1}{2}\right) h\nu_c + \frac{g}{2} h\nu_c m_s - \frac{1}{2} \hbar \delta \left(n + \frac{1}{2} + m_s\right)^2$$

where $m_s = \pm \frac{1}{2}$ and δ is a relativistic correction factor of order 10^{-9} .

For a Dirac point particle, $g = 2$ exactly, and the $|n, m_s = \frac{1}{2}\rangle$ state would be degenerate with the $|n + 1, m_s = -\frac{1}{2}\rangle$ state, to within $\sim \delta$. QED corrections give

g for a real electron a slightly greater value, though, leading to a small difference between spin-up and spin-down states, expressed as an “anomaly frequency” ν_a . Both cyclotron and “anomaly” transitions are driven by RF fields applied to trap electrodes, and a weak coupling between the cyclotron motion and the axial motion allows the direct measurement of the state of the electron by picking up the axial motion with the same electrodes.

All of the properties of this system are extremely well-controlled, enabling the measurement of g to 0.3ppt precision[67, 68]:

$$\frac{g}{2} = 1.001\,159\,652\,180\,73(28) \quad (3)$$

this value, combined with a QED calculation of $g/2$ to tenth order, involving the summing of some 13,000 Feynman diagrams, determines the best measurement of the fine structure constant[69]:

$$\frac{1}{\alpha} = 137.035\,999\,166(34) \quad (4)$$

(where the uncertainty is dominated by the experimental uncertainty in the measurement of g).

The same technique used to measure g for the electron should work to measure g for the positron, improving upon existing tests of CPT symmetry for leptons[70]. A similar method has recently been used to make a direct measurement of the magnetic moment of the proton[71] (which is more technically challenging as the moment is smaller than that of the electron by a factor of $m_p/m_e \sim 1836$), and spin flips of a single trapped proton have been observed[72, 73]. These should lead to high-precision measurements of the proton (and antiproton) g , allowing exceptionally precise QED and CPT tests with hadrons.

4.2. α From Atomic Recoil

Equation 4 is the best measurement to date of the fine-structure constant, but extracting α from g necessarily assumes the correctness of the QED calculation in Ref. [69]. *Testing* QED requires an independent measure of α with which to calculate a theoretical value of g .

We can express α in terms of other well-known constants and the mass m_{Rb} of a rubidium atom:

$$\alpha^2 = \frac{R_\infty m_{Rb} h}{2c m_e m_{Rb}}$$

The Rydberg constant R_∞ and the mass ratio are known to better than ppb accuracy, so an accurate measurement of the ratio h/m_{Rb} enables a direct measurement of α , without any assumptions regarding QED. This ratio is determined from the recoil velocity of a Rb atom absorbing a photon of momentum $\hbar k$:

$$v_r = \frac{\hbar k}{m_{Rb}}$$

The recoil velocity has been measured to ppb accuracy[75] using a Ramsey-Bordé interferometer[74], a variant of the Ramsey interferometry method described in Section 2.1, combined with the Bloch oscillation technique for transferring large amounts of momentum to a sample of atoms.

A sample of ultracold Rb atoms in the $F = 2$ hyperfine ground state are subjected to a $\pi/2$ pulse of a Raman transition that prepares a coherent superposition of $F = 2$ and $F = 1$ hyperfine levels, where the atoms moved to the $F = 1$ state have also acquired a velocity of two photon recoils. Some time later, a second $\pi/2$ pulse is applied, which leads to Ramsey fringes within the velocity distribution of the $F = 1$ atoms. A second pair of $\pi/2$ pulses some time later returns the atoms to the $F = 2$ state, and completes the Ramsey-Bordé interferometer, converting the fringes in the velocity distribution to fringes in the transition probability, as a function of the frequency of the final $\pi/2$ pulses.

In the absence of any other interactions, such an interferometer is sensitive to accelerations or rotations of the atoms during the time between the sets of $\pi/2$ pulses. To measure the recoil velocity, they add an acceleration stage between the $\pi/2$ pulses, illuminating the atoms with a pair of counter-propagating lasers with a frequency offset between them. This can be viewed either as trapping the atoms in an optical lattice that is accelerated as the frequency offset is swept, or as performing a series of N Raman transitions starting and ending in the same internal state, but increasing the velocity by $2v_r$ for each transition. This process is analogous to the Bloch oscillations of an electron in a solid subjected to an electric field.

At the end of the acceleration phase, the atoms have acquired a velocity of $2Nv_r$, leading to a Doppler shift of the final Ramsey-Bordé interference pattern of $\Delta\omega = 2Nkv_r$. Comparing the shift for upward- and downward-accelerated atoms removes the effect of gravity, determining α to 0.66ppb[75, 69]:

$$\frac{1}{\alpha} = 137.035999037(91)$$

Using this value for α to calculate g gives:

$$\frac{g}{2} = 1.001\,159\,652\,181\,82(78)$$

These values agree Eq. 4 and 3, confirming the QED calculation at the ppb level. This accuracy is sufficient to show the contributions of muonic and hadronic terms to the value of g (assuming the correctness of the electron-only parts of QED): a calculation omitting these terms differs from the result of Eq. 4 by roughly 2.5σ [75].

5. Electron EDM

The final class of AMO new physics searches are those seeking a permanent electric dipole moment (EDM) of the electron. Purcell and Ramsey[76] first noted in the 1950's that the existence of a permanent EDM for a fundamental particle would violate time-reversal symmetry: the spin magnetic moment of a particle is odd under time reversal, where an EDM would be even. The existence of a T-violating EDM implies CP-violation elsewhere, assuming CPT symmetry. Known sources of CP-violation within the Standard Model predict EDMs far too small to measure experimentally, in particular, an electron EDM with a magnitude of $d_e \sim 10^{-40} e - cm$. Most theories of physics beyond the Standard Model introduce new sources of CP-violation, though, and predict an electron EDM many orders of magnitude larger: $d_e \sim 10^{-25} - 10^{-30} e - cm$ [77, 78].

The electron EDM cannot be detected with a free electron (which merely moves in response to an electric field), but can lead to small energy shifts in the states of atoms or molecules in an electric field. In the simplest approximation, one would expect

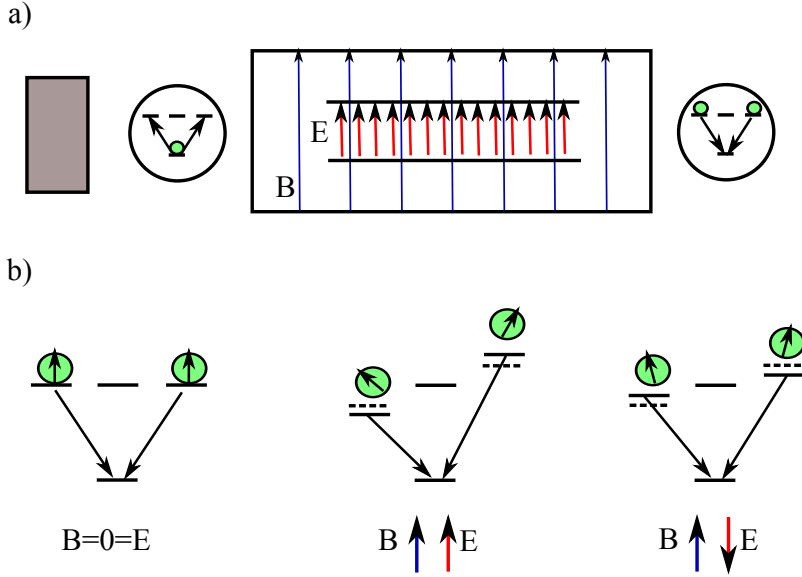


Figure 4. a) Experimental schematic of the electron EDM search. Atoms or molecules are prepared in an initial superposition state, then allowed to evolve freely in a region of uniform electric and magnetic fields. After the free evolution, the probability of returning to the initial state depends on the relative phases of the two parts of the superposition, giving rise to Ramsey fringes. b) Schematic of the interference measurement. In the absence of an applied field (left), the two states in the superposition are degenerate, and remain in phase. With parallel E and B fields (center) the Zeeman shift (dashed line) plus the EDM shift give a phase difference between the two components. Reversing the direction of the E-field (right) does not change the Zeeman shift, but reverses the direction of the EDM shift, changing the phase difference. The resulting change in Ramsey fringes on reversal of the E-field

electrons in an atom to shift so as to cancel an applied electric field, but relativistic effects prevent a perfect cancellation, and for some heavy atoms can even produce an enhancement of the electric field experienced by an electron within an atom. The best atom-based measurement used thallium, where the applied field is enhanced by a factor of ~ 580 [79]. More recent EDM searches use polar molecules, where the internal electric field of the molecule can be orders of magnitude larger than the enhanced field within an atom. The effective field for a recent measurement using YbF[80] molecules was 220 times larger than the field used in the Tl measurement, for a much smaller applied field in the lab.

In both atomic and molecular experiments, the EDM measurement uses a variant of Ramsey interferometry. Rather than preparing a superposition of two different energy states, a beam of atoms or molecules are excited by a “ $\pi/2$ ” pulse to a coherent superposition of two Zeeman sublevels of the same hyperfine state ($F = 1, m_f = 0 \rightarrow F = 1, m_f = \pm 1$ in Tl, and $F = 0, m_f = 0 \rightarrow F = 1, m_f = \pm 1$ in YbF). A uniform magnetic field applied during the free evolution stage creates a phase difference between the two sublevels due to their different Zeeman shifts. This phase difference leads to interference between the two populations when the second “ $\pi/2$ ” pulse attempts to return the population to the initial $m_f = 0$ state, producing Ramsey fringes in the transition probability that are detected with a final state measurement.

To look for an EDM, an electric field is applied either parallel or anti-parallel to the magnetic field. A non-zero electron EDM produces a shift in the energy levels, and thus the interference fringes, that depends on the direction of the E-field. A complete set of measurements consists of many repetitions of the experiment with field directions and magnitudes switched (cycling through 256 combinations of experimental parameters in Tl, and 512 in YbF). Measurements in ^{205}Tl limit $|d_e| \leq 1.6 \times 10^{-27} e - cm$ [79], and YbF provides the best current limit, $|d_e| \leq 1.05 \times 10^{-27} e - cm$ [80].

These measurements already place stringent constraints on theories of physics beyond the Standard Model, ruling out some of the simpler extensions. A sensitivity improvement of another 1-2 orders of magnitude should either definitively detect an electron edm or severely restrict the most popular Standard Model extensions. Such an improvement may be possible in the YbF experiment, for example by cooling the molecular beam source[81], which will dramatically improve the measurement statistics. Another possibility is to move to a different molecule offering better sensitivity; there are numerous such proposals, the most fully developed of which uses thorium monoxide[82]. As of June 2012, the ACME collaboration reports that they are taking preliminary EDM data, and hope improve the YbF limit by an order of magnitude in the near future[83]. Detection of a non-zero electron EDM would imply the existence of new physics at the TeV level, detected using low-energy lasers and modest electric and magnetic fields.

6. Conclusion

The experiments described here represent a small subset of all precision AMO searches for new physics. Numerous other experiments are underway, testing fundamental symmetries with atomic clocks, searching for spin-dependent effects with atomic magnetometers, using atom interferometry to probe gravitational physics, and many others. While it is not possible to describe all of these experiments, the current selection should provide some sense of the potential and the power of precision-based searches for physics beyond the Standard Model.

Acknowledgements

Thanks to Tom Swanson and Dave Phillips for helpful comments on a draft of this article. This article grew out of an invited talk at the 2011 DAMOP meeting.

- [1] T.E. Parker, Proc. 2011 Joint Mtg. IEEE Intl. Freq. Cont. Symp. and EFTF Conf. 596-599 (2011).
- [2] Norman F. Ramsey, Phys. Rev. 78, 695–699 (1950).
- [3] S. T. Cundiff and J. Ye, "Colloquium: Femtosecond optical frequency combs," Reviews of Modern Physics 75, 325 (2003).
- [4] M.C. Stowe, M. J. Thorpe, A. Pe'er, J. Ye, J. E. Stalnaker, V. Gerginov, and S. A. Diddams, Advances in Atomic, Molecular and Optical Physics 55, 1 (2008).
- [5] T. Steinmetz et al., Science 321, 1335-1337 (2008).
- [6] D. F. Phillips et al., Optics Express 20, 13711-13726 (2012).
- [7] J. P. Uzan, Rev. Mod. Phys. 75 (2003) 403 (2003).
- [8] Takeshi Chiba, Prog. Theor. Phys. Vol. 126 No. 6 (2011) pp. 993-1019.
- [9] C. R. Gould, E. I. Sharapov and S. K. Lamoreaux, Phys. Rev. C 74 (2006) 024607.
- [10] Y. Fujii and A. Iwamoto, Phys. Rev. Lett. 91 (2003) 261101.
- [11] C. J. A. Martins et al., Phys. Lett. B 585 (2004) 29.
- [12] E. Menegoni, S. Galli, J. G. Bartlett, C. J. A. Martins and A. Melchiorri, Phys. Rev. D 80 (2009) 087302.
- [13] R.H. Cyburt, B.D. Fields, K.A. Olive, and E.D. Skillman Astropart. Phys. 23 (2005) 313.

- [14] L.L. Cowie and A. Songaila, *Astrophys.J.* 453 (1995) 596.
- [15] Levshakov, S. A., Molaro, P., Lopez, S., D'Odorico, S., Centuri'on, M., Bonifacio, P., Agafonova, I. I., & Reimers, D., 2007, *A&A*, 466, 1077.
- [16] Rahmani, H., et al., arXiv:1206.2653v1.
- [17] Kanekar, N., Chengalur, J. N., & Ghosh, T. 2010, *ApJ*, 716, L23.
- [18] Kanekar, N., Langston, G. I., Stocke, J. T., Carilli, C. L., & Menten, K. L. 2012, *ApJ*, 746, L16
- [19] Levshakov, S. A.; Combes, F.; Boone, F.; Agafonova, I. I.; Reimers, D.; Kozlov, M. G., arXiv:1203.3649v1 (2012).
- [20] J. K. Webb, J. A. King, M. T. Murphy, V. V. Flambaum, R. F. Carswell and M. B. Bainbridge, *Phys. Rev. Lett.* 107 (2011) 191101.
- [21] J. A. King, J. K. Webb, M. T. Murphy, V. V. Flambaum, R. F. Carswell, M. B. Bainbridge, M. R. Wilczynska and F. E. Koch, arXiv:1202.4758.
- [22] Ewan Cameron and Tony Pettitt, arXiv:1207.6223v1 (2012)
- [23] Lea, S. N. 2007 *Rep. Prog. Phys.* 70 1473.
- [24] H. Marion et al., *Phys. Rev. Lett.* 90, 150801 (2003).
- [25] Guéna, J. et al., <http://arxiv.org/abs/1205.4235v1>.
- [26] N. Ashby et al., *Phys. Rev. Lett.* 98, 070802 (2007).
- [27] J. C. Berengut, V. V. Flambaum, arXiv:1008.3957v1 (2010).
- [28] S.A. Diddams, Th. Udem, J.C. Bergquist, E.A. Curtis, R.E. Drullinger, L. Hollberg, W.M. Itano, W.D. Lee, C.W. Oates, K.R. Vogel, and D.J. Wineland An Optical Clock Based on a Single Trapped Hg^+ Ion *Science* 293 825-293 (2001).
- [29] Chr. Tamm, S. Weyers, B. Lipphardt, and E. Peik, *Phys. Rev. A* 80, 043403 (2009).
- [30] Huntemann, N. et al., *Phys. Rev. Lett.* 108, 090801 (2012).
- [31] Margolis, H. S. et al. *Science* 19, 1355 (2004).
- [32] Y. H. Wang, T. Liu, R. Dumke, A. Stejskal and Y. N. Zhao, et al. *Laser Physics* 17, 1017-1024 (2007).
- [33] Kajita, M. et al., *Phys. Rev. A* 72, 043404 (2005).
- [34] P Gill et al. *Meas. Sci. Technol.* 14 1174 (2003).
- [35] E. Peik et al., *Phys. Rev. Lett.* 93, 170801 (2004).
- [36] T. Fortier et al., *Phys. Rev. Lett.* 98 070801 (2007).
- [37] P. O. Schmidt et al., *Science* 309, 749 (2005).
- [38] T. Rosenband, P.O. Schmidt, D. Hume, W.M. Itano, T. Fortier, J. Stalnaker, K. Kim, S.A. Diddams, J. Koelemeij, J.C. Bergquist, and D.J. Wineland Observation of the $^1\text{S}_0$ - $^3\text{P}_0$ Clock Transition in $^{27}\text{Al}^+$ *Phys. Rev. Lett.* 98 220801-4 (2007).
- [39] T. Rosenband, D.B. Hume, P.O. Schmidt, C.W. Chou, A. Brusch, L. Lorini, W.H. Oskay, R.E. Drullinger, T.M. Fortier, J.E. Stalnaker, S.A. Diddams, W.C. Swann, N.R. Newbury, W.M. Itano, D.J. Wineland, and J.C. Bergquist Frequency Ratio of Al^+ and Hg^+ Single-Ion Optical Clocks; Metrology at the 17th Decimal Place *Science* 319 1808 (2008).
- [40] C. W. Chou, D. B. Hume, J. C. J. Koelemeij, D. J. Wineland, T. Rosenband, *Phys. Rev. Lett.* 104, 070802 (2010).
- [41] C. W. Chou, D. B. Hume, D. J. Wineland, and T. Rosenband, *Science* 329, 1630 (2010).
- [42] Predehl, K.; Grosche, G.; Raupach, S. M. F.; Droste, S.; Terra, O.; Alnis, J.; Legero, Th.; Hänsch, T. W.; Udem, Th.; Holzwarth, R.; Schnatz, H., *Science*, Volume 336, Issue 6080, pp. 441- (2012).
- [43] A. Derevianko and H. Katori, *Rev. Mod. Phys.* 83, 331–347 (2011).
- [44] Takamoto, M. et al., *Nature* 435, 321 (2005)
- [45] Ludlow, A. D. et al., *Phys. Rev. Lett.* 96, 033003 (2006).
- [46] Le Target, R. et al. *Phys. Rev. Lett.* 97, 130801 (2006)
- [47] Kohno, T., M. Yasuda, K. Hosaka, H. Inaba, Y. Nakajima, and F.-L. Hong, *Appl. Phys. Express* 2(7), 072501 (2009).
- [48] Lemke, N. D., et al. *Phys. Rev. Lett.* 103, 063001 (2009).
- [49] Hachisu, H. et al., *Phys. Rev. Lett.* 100, 053001 (2008).
- [50] Petersen, M. et al., *Phys. Rev. Lett.* 101, 183004 (2008).
- [51] McFerran, J. J. et al., *Phys. Rev. Lett.* 108, 183004 (2012).
- [52] S. Blatt, A. D. Ludlow, G. K. Campbell, J. W. Thomsen, T. Zelevinsky, M. M. Boyd, J. Ye, X. Baillard, M. Fouché, R. Le Targat, A. Brusch, P. Lemonde, M. Takamoto, F.-L. Hong, H. Katori, V. V. Flambaum, *Phys. Rev. Lett.* 100, 140801 (2008).
- [53] E. Peik and C. Tamm, *Europhys. Lett.* 61 181 (2003).
- [54] Campbell, C. J. et al., *Phys. Rev. Lett.* 108, 120802 (2012).
- [55] Campbell, C. J. et al., *Phys. Rev. Lett.* 102, 233004 (2009).
- [56] Kazakov, G. A. et al., arXiv:1204.3268v2 [physics.atom-ph] (2012).

- [57] Litvinova, E. et al., Phys. Rev. C 79, 064303 (2009).
- [58] V. A. Dzuba, V. V. Flambaum, and J. K. Webb, Phys. Rev. A 59, 230 (1999)
- [59] Cingöz, A. et al., Phys. Rev. Lett. 98, 040801 (2007).
- [60] Ferrell, S. J. et al., Phys. Rev. A 76, 062104 (2007).
- [61] Nguyen, A. T. et al., Phys. Rev. A 69, 022105 (2004).
- [62] Lu, M. et al., Phys. Rev. Lett. 107, 190401 (2011).
- [63] Lu, M. et al., Phys. Rev. Lett. 108, 215301 (2012).
- [64] Berengut, J. C. et al., Phys. Rev. A 84, 054501 (2011).
- [65] Berengut, J. C. et al., arXiv:1206.0534v1 (2012).
- [66] Lowell S. Brown and Gerald Gabrielse Rev. Mod. Phys. 58, 233–311 (1986).
- [67] Hanneke, D. et al., Phys. Rev. Lett. 100, 120801 (2008).
- [68] Hanneke, D. et al., Phys. Rev. A 83, 052122 (2011).
- [69] Aoyama, T. et al., arXiv:1205.5368v1 (2012).
- [70] R. S. Van Dyck Jr., P. B. Schwinberg, and H. G. Dehmelt, Phys. Rev. Lett. 59, 26 (1987).
- [71] DiSciaccia, J. and Gabrielse, G, Phys. Rev. Lett. 108, 153001 (2012).
- [72] Ulmer, S. et al., Phys. Rev. Lett. 106, 253001 (2011).
- [73] Rodegheri, C. C. et al., New J. Phys. 14 063011 (2012).
- [74] Ch. J. Bordé, Phys. Lett. A 140, 10 (1989).
- [75] Bouchendira, R. et al., Phys. Rev. Lett. 106, 080801 (2011).
- [76] E.M.Purcell, N.F.Ramsey, Phys. Rev. 78, 807 (1950).
- [77] W. Bernreuther and M. Suzuki, Rev. Mod. Phys. 63, 313 (1991).
- [78] Ritz, A., Nuclear Instruments and Methods in Physics Research A, 611, 117 (2009).
- [79] Regan, B. C., et al., Phys. Rev. Lett. 88, 071805 (2002).
- [80] Hudson, J. J. et al., Nature 473, 493 (2011).
- [81] Skoff, S. M. et al., Phys. Rev. A 83, 023418 (2011).
- [82] A C Vutha et al. J. Phys. B: At. Mol. Opt. Phys. 43 074007 (2010).
- [83] D. DeMille, private communication.